Adam ZIELIŃSKI

Instytut Metalurgii Żelaza

Grzegorz GOLAŃSKI

Czestochowa University of Technology

Paweł URBAŃCZYK

Office of Technical Inspection

Jacek SŁANIA, Joanna JASAK

Czestochowa University of Technology

MICROSTRUCTURE AND PROPERTIES OF DISSIMILAR WELDED JOINT BETWEEN P91 AND TP347HFG STEELS AFTER 105 000 H SERVICE

This paper presents the results of investigations of a dissimilar welded joint made between X10CrMoVNb9-1 (P91) martensitic steel and TP347HFG austenitic steel. The welded joint material was taken from a primary steam superheater coil operated at maximum working temperature of approx. 540°C for more than 105 000 hours. Destructive testing and metallographic tests were carried out for the welded joint material to determine the impact of long-term service on the properties of the joint. Microstructure of the welded joint was observed using a optical microscope (OM) and scanning electron microscope (SEM). The destructive testing included: impact test, static tensile test and hardness measurement.

Key words: microstructure, mechanical properties, welded joint P91 / TP347HFG

MIKROSTRUKTURA I WŁAŚCIWOŚCI RÓŻNOIMIENNEGO ZŁĄCZA SPAWANEGO POMIĘDZY STALĄ P91 I TP347HFG PO 105 000 GODZIN EKSPLOATACJI

W pracy zostały przedstawione wyniki badań złącza spawanego różnoimiennego, wykonanego pomiędzy stalą martenzytyczną w gatunku X10CrMoVNb9-1 (P91), a stalą austenityczną TP347HFG. Materiał złącza spawanego został pobrany z wężownicy przegrzewacza pary świeżej, pracującego w maksymalnej temperaturze pracy około 540°C w czasie ponad 105 000 godzin. Dla materiału złącza spawanego przeprowadzono badania niszczące oraz badania metalograficzne, w celu określenia wpływu długotrwałej eksploatacji na właściwości złącza. Obserwacji mikrostruktury złącza spawanego dokonano za pomocą mikroskopu świetlnego (OM) oraz elektronowego mikroskopu skaningowego (SEM). Badania niszczące obejmowały: próbę udarności, statyczną próbę rozciągania oraz pomiar twardości.

Słowa kluczowe: mikrostruktura, właściwości mechaniczne, złącze spawane P91 / TP347HFG

1. INTRODUCTION

At present, the biggest investments in the power industry with regard to construction of power units are based on the use of technologies for generation of steam with supercritical parameters. Such units are in compliance with regulations introduced by UE directives concerning the emission of harmful compounds into the atmosphere and at the same time maintain high efficiency of electric energy generation.

The use of steam generation technology based on supercritical parameters involves the increase in working parameters of the pressure elements of power boiler, in particular heating areas of steam superheaters.

The operation of boiler's pressure elements in the high range of thermal and mechanical loads requires the use of high-temperature creep resisting construction materials with increased creep strength as well as advanced technologies for joining these materials.

Materials that meet the above criteria include creep resisting ferritic (martensitic, bainitic) steels and increasingly used austenitic steels, or else nickel-base superalloys, which are in the course of being introduced for production.

One of the methods for improvement in high-temperature creep resistance and creep strength of steels used in the power industry is to raise the content of chromium and introduce the alloying elements such as: molybdenum, vanadium, niobium and nitrogen [1]. The material that belongs to this group is X10CrMoVNb9-1 (P91) steel with martensitic structure.

This steel has very good strength properties, while at the same time it keeps suitable plasticity and ductility.

Lower carbon content in steel of this type affects the reduction in martensite hardness, which has direct impact on the increase in ductility and allows cooling an element after welding to room temperature without the risk of cold cracking [1]. Steels in this group are dedicated to work within the range of temperatures up to 650°C [1–4].

Problems and limitations concerning the use of new grades of bainitic and martensitic steels for manufacturing strongly loaded pressure elements of steam boilers in the power industry have contributed to the interest in creep resisting austenitic steels or nickel-base alloys [4–8].

Recommended for manufacturing the pressure elements of power boilers operated in the temperature range of 650÷700°C are 18-8 type austenitic steels or nickel-base alloys (up to approx. 750°C) [1, 3, 4].

However, the use of austenitic steels presents a number of problems due to their physical properties such as: low thermal conductivity and high coefficient of linear expansion. These properties make technological problems appear during the manufacture of pressure elements of steam boilers. In particular, it concerns joining by welding of austenitic steels with martensitic steels due to the occurrence of material heterogeneity in the welded joint.

Due to differences in chemical composition, thermal expansion and creep strength between two joined steels, dissimilar welded joints are exposed to the risk of damages [9].

In case of welding of steels that differ in chemical compositions, structural heterogeneities may occur on the line of fusion of the welded joint at the points of their joining, during heat treatment or during the operation at elevated temperature. Welding of materials with different chemical compositions may result in the occurrence of coarse-grained decarburised ferritic zone with low hardness on one side of the line of fusion and hard carburised zone on the other side, which is caused by the formation and growth of carbides. The mechanism responsible for the formation of the abovementioned lines of fusion in dissimilar welded joints is carbon diffusion [1, 9, 10].

Carbon diffusion takes place from the areas with lower content of carbide-forming elements with higher carbon potential towards the areas with lower carbon potential (higher content of carbide-forming elements). One of the methods for preventing the occurrence of both zones on the line of fusion while welding of steels with different chemical compositions is to use additional nickel-based materials or create a buffer zone when using them [1].

2. RESEARCH METHODOLOGY

The investigations of microstructure were performed on prepared metallographic microsections (acc. to PN-EN ISO 17639:2013). Due to different structure of base materials of the joint, it was necessary to use different reagents to the disclosure of metallographic microstructure: TP347HFG steel – Mi19Fe, P91 steel – ferrous chloride, weld – electrolytic etching.

The microstructure images were observed and recorded using Axiovert 25 optical microscope (OM) and JOEL JSM 6610LV scanning electron microscope (SEM).

Mechanical properties of the tested steels were determined at room temperature using the following equipment: static tensile test – MTS-810 tensile testing machine (acc. to PN-EN ISO 6892-1 [11]), Vickers hardness measurement – Future – Tech FV – 700 hardness testing machine (acc. to PN-EN ISO 6507-1 [12]), impact test KV_2 300/5 (impact energy strength determined on test pieces of width reduced to 5 mm, striking edge radius of 2 mm, impact testing initial energy of 300 J) on V-notched Charpy specimens with reduced dimensions of 5×10×55 (acc. to PN-EN ISO 148-1 [13]). The results of mechanical tests are the mean value of three measurements.

The analysis of chemical composition of the parent materials was carried out with spark spectrometer and of the weld – using SEM+EDS technique.

3. MATERIAL FOR INVESTIGATIONS

The subject of the investigations was dissimilar welded joint taken from a coil of steam superheater that was operated for more than 105 000 hours at steam pressure of 12.5 MPa and approx. 540°C.

Chemical composition of base materials, i.e. P91 and TP347HFG steels, is presented in Tables 1 and 2, respectively.

Table 1. Chemical composition of the P91 steel, wt%

Tabela 1. Skład chemiczny stali P91, % wag.

C	Mn	Si	P	S	Cr	Mo	Ni	V	N
0.13	0.46	0.34	0.017	0.005	8.83	0.99	0.27	0.21	0.064

Table 2. Chemical composition of the TP347HFG steel, wt%

Tabela 2. Skład chemiczny stali TP347HFG, % wag.

C	Mn	Si	P	S	Cr	Ni	Nb	N
0.09	1.56	0.47	0.023	0.003	18.38	11.99	0.61	0.04

The analysis of chemical composition of the joint showed that it had been welded using two different additional materials. On the weld root side the additional material for welding of austenitic steels was used, while on the weld face side it was the nickel-based additional material. The chemical composition of additional materials is presented in table 3.

Table 3. Chemical composition of the additional material on the weld face side and the weld root side, wt%

Tabela 3. Skład chemiczny materiału dodatkowego od strony lica i grani, % wag.

	Ni	Cr	Fe	Mn	Nb	Ti	Si
FACE	61.15	18.30	15.47	2.51	2.12	0.27	0.19
ROOT	31.95	17.23	46.92	1.95	1.53	–	0.42

The macroscopic view of the welded joint is presented in Fig. 1.

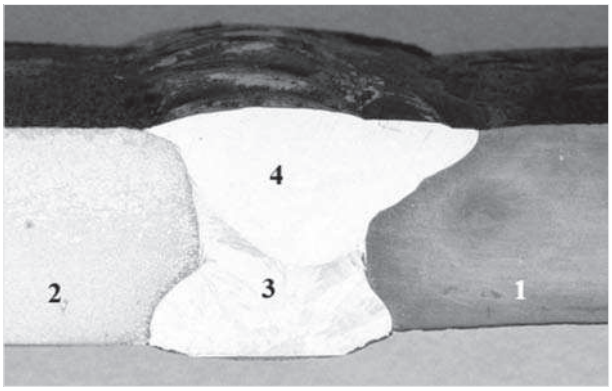

Fig. 1. Macrostructure of welded joint: 1 – P91 steel, 2 – TP347HFG steel, 3 – root, 4 – face

Rys. 1. Makrostruktura złącza spawanego: 1 – stal P91, 2 – stal TP347HFG, 3 – grań, 4 – lico

4. RESULTS OF INVESTIGATIONS

4.1. MICROSTRUCTURE OF TP347HFG STEEL AFTER SERVICE

The microstructure of the TP347HFG steel after service consisted of austenite grains with visible annealing twins and numerous precipitations distributed both at the grain boundaries and in the matrix (Fig. 2).

In the microstructure, the presence of large precipitations distributed in strips within matrix was found. Numerous austenite grains with slip lines were observed too.

The size of austenite grain in the tested steel, determined by means of drawing patterns in accordance with ASTM scale, was 8/7. The fine-grained microstructure of the TP347HFG steel (grain size $\geq$ 8) provides high oxidation resistance and higher plasticity (represented by elongation in creep tests) at creep resistance comparable to that of brittle timber steels [3, 5].

The fine-grained microstructure of the TP347HFG steel has also direct impact on slower decrease in impact energy during long-term service [3, 5, 14].

Identifications performed in the tested TP347HFG steel revealed the occurrence of two types of NbC precipitations inside grains: a) large primary carbides and b) fine-dispersive secondary precipitations.

Due to their sizes, the large primary NbC precipitations do not affect the increase in precipitation hardening of austenitic steels, but they contribute to the binding of carbon, thus reducing the precipitation of $M_{23}C_6$ carbides [3, 5]. The primary niobium carbides are considered to be disadvantageous precipitations as nucleation and development of creep cracking may come about at the carbide/matrix interface [5, 15].

The fine-dispersive NbC niobium carbides are mainly precipitated at dislocations or stacking faults. They contribute to the increase in strength properties and creep resistance [14, 15]. On the other hand, the $M_{23}C_6$ carbide precipitations were revealed at the grain boundaries. No precipitations were observed at the twin boundaries in the tested steel.

The identifications performed did not reveal the occurrence of precipitations of intermetallic phases, such as: σ, G, Z phase etc, in the tested steels, which can be explained by low service temperature.

4.2. MICROSTRUCTURE OF P91 STEEL AFTER SERVICE

The P91 steel, after heat treatment including austenitising with air-cooling followed by high-temperature tempering, reveals the tempered martensite structure with $M_{23}C_6$ and MC carbides [5]. The microstructure of the tested steel after service showed insignificant decomposition of tempered martensite related to numerous precipitations of different size in the form of chains at the boundaries of initial austenite grains. Preserved lath nature was visible in the microstructure of the tested steel (Fig. 3).

4.3. MACROSTRUCTURE OF WELDED JOINT

4.3.1. Microstructure of HAZ in TP347HFG steel

The microstructure in the joint – within the heat-affected zone (HAZ) in the vicinity of the line of fusion of the TP347HFG steel, was the austenitic microstructure characterised by large grain of 3/4 according to the ASTM scale (Fig. 4).

In this area, numerous fine precipitations forming the so-called continuous network of precipitations

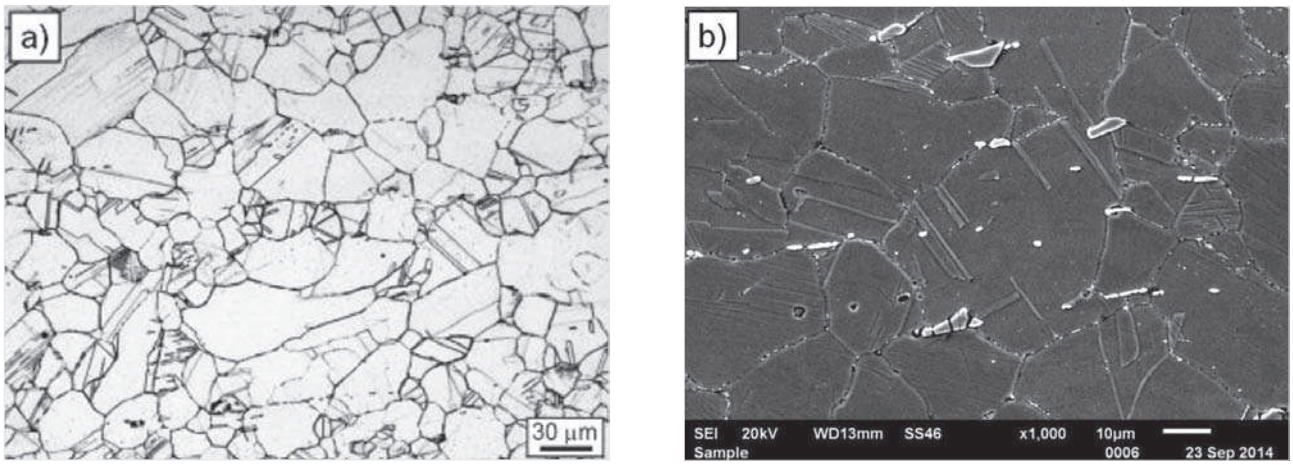

Fig. 2. Microstructure of TP347HFG steel after service: a) OM, b) SEM

Rys. 2. Mikrostruktura stali TP347HFG po eksploatacji: a) OM, b) SEM

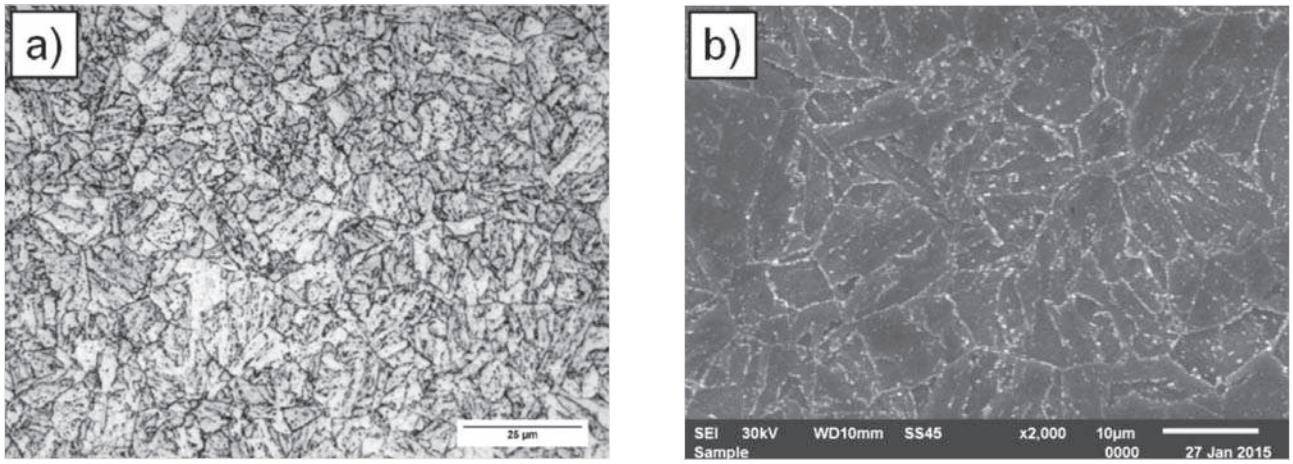

Fig. 3. Microstructure of P91 steel after service: a) OM, b) SEM

Rys. 3. Mikrostruktura stali P91 po eksploatacji: a) OM, b) SEM

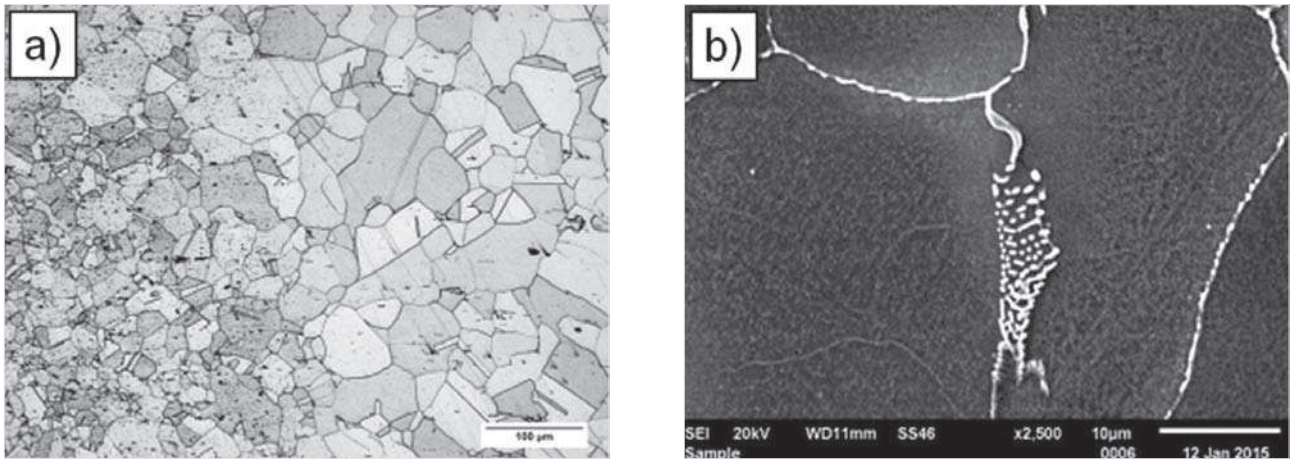

Fig. 4. Microstructure of welded joint within HAZ in the vicinity of the line of fusion on the TP347HFG steel side; a) OM, b) SEM

Rys. 4. Mikrostruktura złącza spawanego w SWC w pobliżu linii wtopienia od strony materiału TP347HFG; a) OM, b) SEM

were visible at the grain boundaries, while both inside grains and at their boundaries carbide eutectics were observed. The influence of heat from welding results in dissolution of primary NbC carbides in the matrix, which are precipitated again in the form of carbide eutectic or in the form of intermetallic phase due to quick crystallisation [16].

4.3.2. Microstructure of HAZ in P91 steel

In principle, two areas can be distinguished in the microstructure of the P91 steel. In the vicinity of the line of fusion, HAZ with coarse-grained structure (CG-HAZ – Coarse Grain Heat Affected Zone) and numerous precipitations of different size were observed. These precipitations were observed at the former austenite grain boundaries, at the lath boundaries and inside grains. In places, the number of precipitations was so large that it assumed the form of the so-called continuous network at the grain boundaries (Fig. 5).

The second HAZ in the P91 steel is an area characterised by fine-grained structure – (FGHAZ – Fine Grain Heat Affected Zone) (Fig. 6). In this area, the significant degree of microstructure degradation, manifesting itself in the occurrence of microstructure consisting of ferrite and precipitations, was found. At the ferrite grain and former austenite grain boundaries, the numerous large precipitations form the so-called "continuous network of precipitations" in places. The advanced degree of microstructure degradation is connected with multiple tempering of this HAZ. The degraded microstructure of the P91 steel in FGHAZ may contribute to faster damage to this area of the welded joint as a result of advanced precipitation processes (coagulation of $M_{23}C_6$ carbides, precipitation and growth of the Laves phase) and decay of the lath microstructure. Damages in this area of the welded joint are called type IV damages [17].

In the line of fusion of the P91 steel, the occurrence of carburised layer was observed in the weld on its root side (Fig. 7). The occurrence of this layer is connected with carbon diffusion from the areas with lower content of carbide-forming elements towards the areas with the number of these elements is higher (the so-called chromium potential is higher) [1]. In consequence, the carbon separation process may result in the formation of soft layer – a decarburised zone characterised by coarse-grained structure with low hardness and tensile strength. The presence of this layer has a very significant impact on the reduction in creep resistance, fatigue strength, and in particular to thermal fatigue [10]. This layer was not observed on the line of fusion on the face side (Fig. 8).

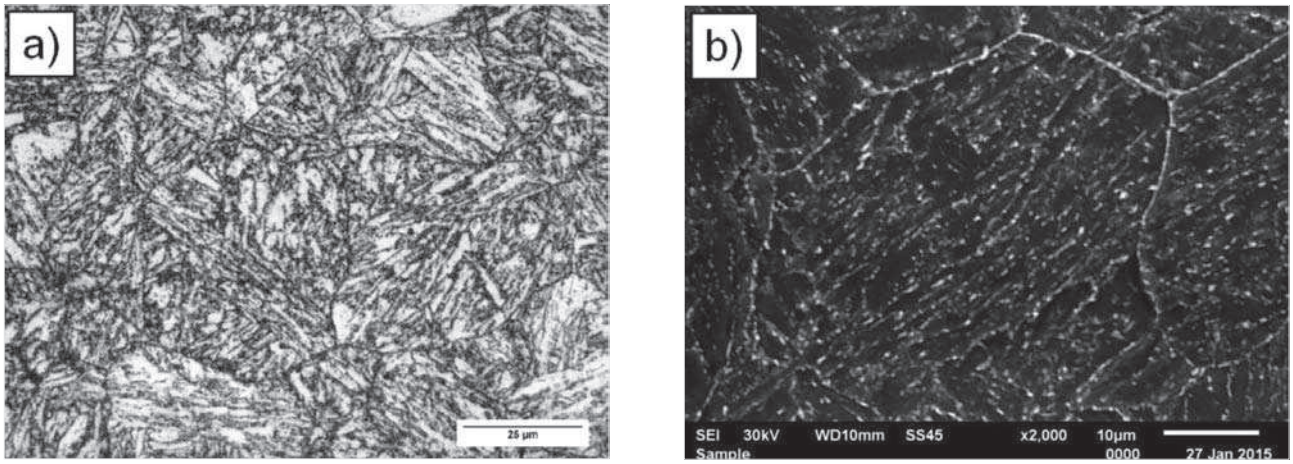

Fig. 5. Microstructure of welded joint within coarse grained HAZ (CGHAZ) on the line of fusion on the P91 steel side; a) OM, b) SEM

Rys. 5 Mikrostruktura złącza spawanego w obszarach gruboziarnistych SWC (CGHAZ) na linii wtopienia od strony materiału P91 a) OM, b) SEM

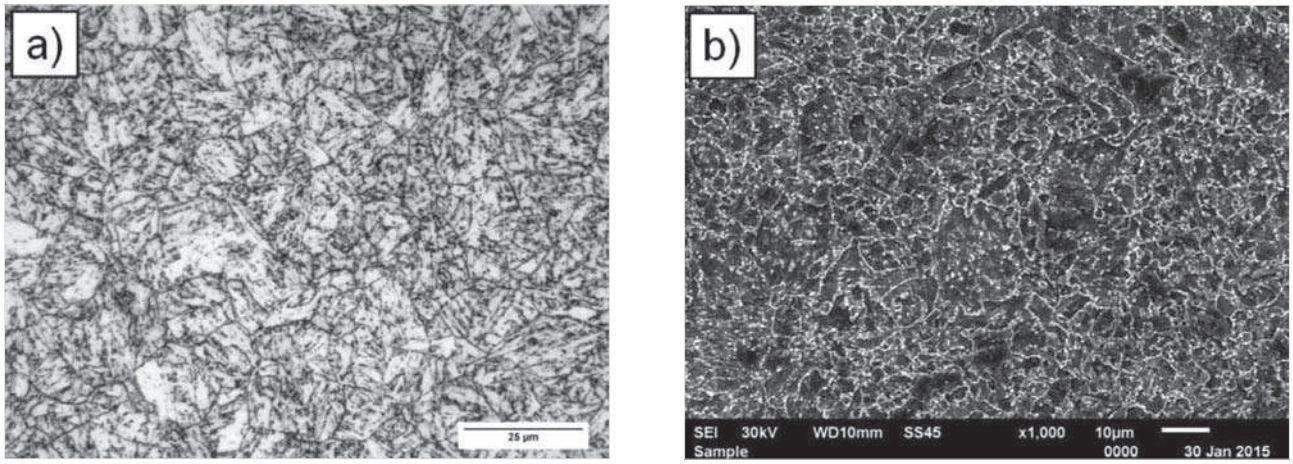

Fig. 6. Microstructure of welded joint within fine grained HAZ (FGHAZ) on the line of fusion on the P91 material side; a) OM, b) SEM

Rys. 6. Mikrostruktura złącza spawanego w obszarach drobnoziarnistych SWC (FGHAZ) od strony materiału P91 a) OM, b) SEM

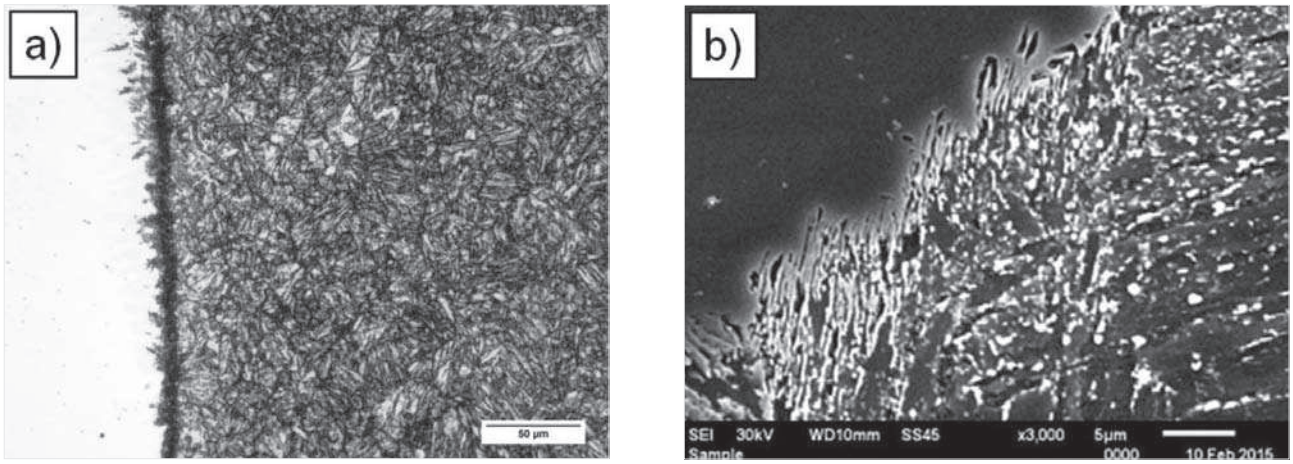

Fig. 7. Microstructure of welded joint on the line of fusion on the P91 steel side (root of weld); a) OM, b) SEM

Rys. 7. Mikrostruktura złącza spawanego na linii wtopienia od strony materiału P91 (grań spoiny); a) OM, b) SEM

In addition, the occurrence of non-mixed areas, manifesting themselves in characteristic "tongues", were observed directly at the line of fusion. Their occurrence is caused by the presence of stationary liquid layer (the so-called Nernst's layer), adjacent to the line of fusion, in the pool during welding [1] – (Fig. 9).

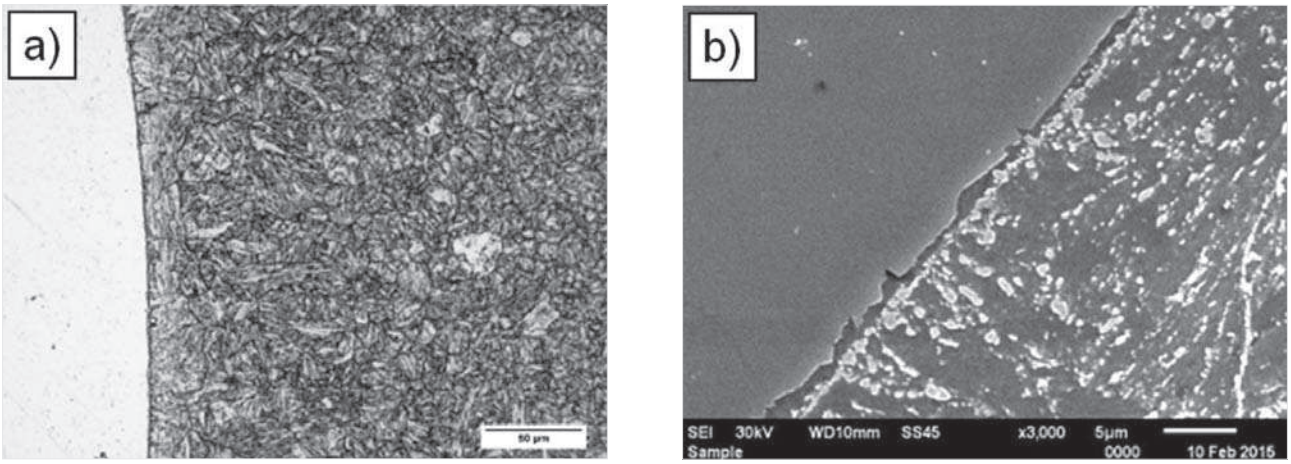

Fig. 8. Microstructure of welded joint on the line of fusion on the P91 steel side (face of weld); a) OM, b) SEM

Rys. 8.Mikrostruktura złącza spawanego na linii wtopienia od strony materiału P91 (lico spoiny); a) OM, b) SEM

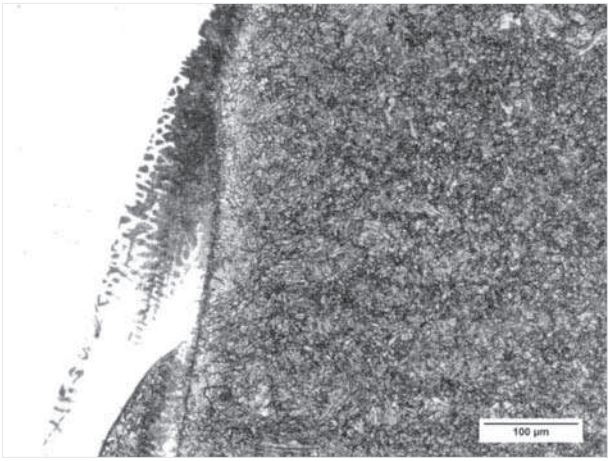

Fig. 9. Heterogeneity of chemical composition of the weld in the form of characteristic "tongues"

Rys. 9. Niejednorodność składu chemicznego spoiny w postaci charakterystycznych „języków"

4.4. MICROSTRUCTURE OF WELDED JOINT – WELD

In the weld, the epitaxial crystallisation was observed on its face side (Fig. 10a), while on the root side – the cellar-dendritic crystallisation (Fig. 10b). The direction of crystallite growth in the weld on its root side was different in individual weld areas.

4.5. MECHANICAL PROPERTIES OF WELDED JOINT

The welding process and operation affected the change in properties of the dissimilar welded joint. The performed KV_2 300/5 impact tests revealed that the lowest impact energy was demonstrated by HAZ in the P91 steel (Table 4). It results mainly from the micro-

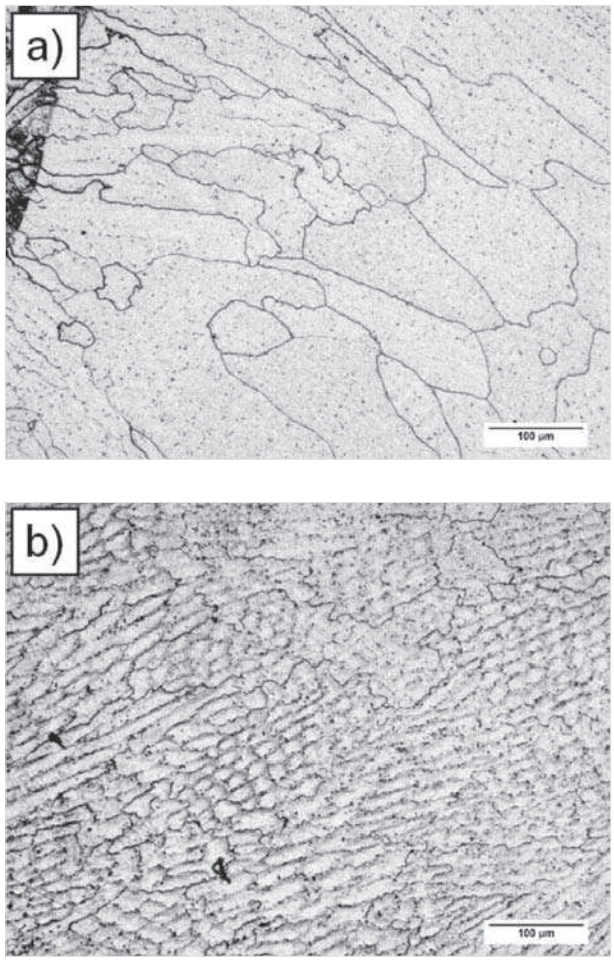

Fig. 10. Microstructure of welded joint: a) weld on its face side; b) weld on its root side

Rys. 10. Mikrostruktura złącza spawanego: a) spoina od strony lica; b) spoina od strony grani

Table 4. Results of impact energy of the joint

Tablica 4. Wyniki badania właściwości mechanicznych złącza

Impact energy									
MR_P91		SWC_P91		Weld		SWC_347		MR_347	
J	J/cm^2	J	J/cm^2	J	J/cm^2	J	J/cm^2	J	J/cm^2
49	122.5	19	47.5	33	82.5	39	97.5	42	105

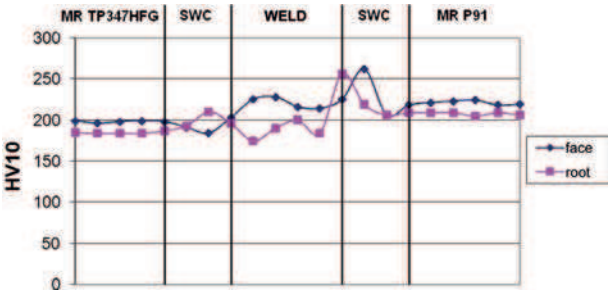

Fig. 11. Hardness distribution in the welded joint
Rys. 11. Rozkład twardości w złączu spawanym

structure degradation in these areas, which manifests itself in: decay of lath martensitic microstructure and advanced precipitation processes (Fig. 5 and 6).

Tensile strength of the joint was 610 MPa and rupture took place beyond the weld in the line of fusion on the martensitic steel side. The obtained value of strength does not meet the acceptance criterion adopted in accordance with the product standard for P91 steel, and the rupture itself took place beyond the weld.

The hardness distribution in the tested joint is shown in Fig. 11.

5. SUMMARY

The performed metallographic tests and investigations of mechanical properties revealed insignificant degree of degradation of the microstructure of base materials and HAZ on the TP347HFG steel side. The most degraded area was HAZ on the P91 steel side. In the fine-grained area of HAZ (FGHAZ), the P91 steel was characterised by complete decomposition of martensite lath structure in favour of ferrite microstructure with numerous precipitations. The obtaining of so much degraded microstructure to a large extent results from multiple high-temperature tempering of this area during technological operations: during production of material (tube), during welding as a result of the impact of temperature from solidifying weld pool, and as a result of heat treatment of the welded joint. The above-mentioned changes in the microstructure contribute to accelerated damage to this area during service. In consequence, it results in cracking named type IV cracking.

Due to the occurrence of strongly degraded microstructure of the welded joint within FGHAZ on the P91 steel side, the possibility of applying the post-weld treatment of 9%Cr steel in the lower acceptable range of annealing temperature should be considered.

Within the area of the line of fusion of the P91 steel, the occurrence of carburised zone related to carbon diffusion from the P91 steel to the weld with composition corresponding to that of the austenitic steel was observed on the root side of the welded joint. However, the carburised zone was not observed on the line of fusion on the face side of the joint, which is caused by the use of nickel-based additional material.

REFERENCE

1. Tasak E., Ziewiec A.: Weldability of construction materials. Volume I. Weldability of steels, Wydawnictwo JAK – Krakow 2009
2. Pikos I., Kocurek R., Adamiec J.: Perspectives of materials for fin tubes, Advances in material science, vol. 13, No. 3 (37), p. 17-25
3. Zheng-Fei H.: Heat-resistant Steels, Microstructure Evolution and Life Assessment in Power Plants, Thermal Power Plants, InTech Publ. 2012, p. 195-226
4. Brózda J.: New-generation austenitic steels used for power equipment with supercritical parameters and their welding, Bulletin of the Polish Welding Centre of Excellence. 5 (2006), p. 40-48
5. Golański G., Kolan C., Jasak J., Urbańczyk P., Słania J., Zieliński A.: Microstructure and mechanical properties of TP347HFG steel after long-term service, Energetyka. 11 (2014), p. 655-657
6. Golański G., Kępa J.: Role of complex nitride Cr(V, Nb)N – Z phase in high-chromium martensitic steels, Inżynieria Materiałowa. 5 (2011), p. 917-922
7. Golański G., Jasak J., Słania J.: Microstructure, properties and welding of T24 steel – critical review, Kovove Mater. 52 (2014) 99-106
8. Iseda A., Okada H., Semba H., Igarashi M.: Long-term creep properties and microstructure of Super304H, TP347HFG and HR3C for advanced USC boilers, in: R. Viswanathan, D. Gandy, K. Coleman (Eds.) Advances in Materials Technology for Fossil Power Plants Proceedings from the Fifth International Conference, Macro Island, 2007, p. 185-196
9. Brentrup G.J., DuPont J. N.: Fabrication and Characterization of Graded Transition Joints for Welding Dissimilar Alloys, Welding Journal, vol. 92 (2013), p. 72-79
10. Tasak E., Ziewiec A., Ziewiec K.: Problems during welding and repair to joints of dissimilar steel, Archives of Foundry, 6, 21, 2006, 221-227
11. Polish Norm PN-EN ISO 6892-1:2009, Metallic materials. Tensile testing. Part 1 – Method of test at room temperature. Polish Committee for Standardisation
12. Polish Norm PN-EN ISO 6507-1: 2007, Metallic materials. Vickers hardness test. Part 1 – Test method. Polish Committee for Standardisation
13. Polish Norm PN-EN ISO 148-1: 2010, Metallic materials. Charpy impact test. Part 1 – Test method. Polish Committee for Standardisation
14. Yoshikawa K., Teranishi H., Tokimasa K., Fujikawa H., Miura M., Kubota K.: Fabrication and properties of corrosion resistant TP347H stainless steel, J. Mater. Eng. 10, 1 (1988) 69-84
15. Chengyu C., Hongyao Y., Xishan X.: Advanced austenitic heat-resistant steels for ultra-super-critical (USC) fossil power plants, Alloy steel – properties and use, InTech Publ. 2011, p. 171-200
16. Jeng S.L., Lee H.T., Rehbach W.P., Kuo T.Y., Weirich T. E., Mayer J. P.: Effect of Nb on microstructure and corrosive property in the Alloy 690 – SUS 304L weldment, Mater. Sc. Eng. A, 397, 2009, p. 229-238
17. Goyal S., Laha K., Chandravathi K.S., Bhanu Sankara Rao K.: Prediction of type IV cracking behavior of 2.25Cr-1Mo steel weld joint based on finite element analysis, Transactions of the Indian Institute of Metals, vol. 63 (2010), p. 461-466